Supporting Information

Importance of Out-of-State Spin-Orbit Coupling for Slow Magnetic Relaxation in Mononuclear Fe^{II} complexes.

Po-Heng Lin,[a,b] Nathan C. Smythe,[c] Serge I. Gorelsky,[a,b] Steven Maguire,[a,b] Neil J. Henson,[d] Ilia Korobkov,[a] Brian L. Scott,[e] John C. Gordon,[c] R. Tom Baker,[a,b] Muralee Murugesu*[a,b]

[a] Department of Chemistry, University of Ottawa, 10 Marie Curie, Ottawa, ON, K1N 6N5, Canada.

[b] Centre for Catalysis Research and Innovation (CCRI), 30 Marie Curie, Ottawa, ON, K1N 6N5, Canada.

[c] Chemistry Division, Los Alamos National Laboratory, MS J582, Los Alamos, NM 87545.

[d] Theoretical Division, Los Alamos National Laboratory, MS B268, Los Alamos, NM 87545.

[e] Materials Physics and Applications Division, Los Alamos National Laboratory, MS J514, Los Alamos, NM 87545

m.murugesu@uottawa.ca

Experimental part:

General:

All manipulations were performed in an Ar-filled glovebox. Anhydrous solvents were obtained from Aldrich or Acros and stored over 4 Å molecular sieves under an Ar atmosphere in a glovebox. $FeBr_2$, $KN(SiMe_3)_2$ (Aldrich), $FeCl_2$, depe and PCy_3 (Strem) were purchased commercially and used as received. Elemental analyses were performed by Atlantic Microlab (Norcross, GA) or Guelph Chemical Laboratories and Chemisar Laboratories, Inc. (Guelph, ON, Canada). A crystal of **1** was mounted in a nylon cryoloop from Paratone-N oil under argon gas flow. The data was collected on a Bruker D8 diffractometer, with APEX II charge-coupled-device (CCD) detector, and Bruker Kryoflex low temperature device. The instrument was equipped with graphite monochromatized MoKα X-ray source (λ= 0.71073 Å), and a 0.5 mm monocapillary. A hemisphere of data was collected using ω scans, with 10-second frame exposures and 0.5° frame widths. Data collection and initial indexing and cell refinement were handled using APEX II[1] software. Frame integration, including Lorentz-polarization corrections, and final cell parameter calculations were carried out using SAINT+[2] software. The data were corrected for absorption using redundant reflections and the SADABS[3] program. Decay of reflection intensity was not observed as monitored *via* analysis of redundant frames. The structure was solved using Direct methods and

difference Fourier techniques. All hydrogen atom positions were idealized, and rode on the atom they were attached to. The final refinement included anisotropic temperature factors on all non-hydrogen atoms. For **1**, two disordered carbon atoms in a cyclohexyl ring were each modeled in two one-half occupancy positions, and hydrogen atom positions were not included for the disordered atoms. Structure solution, refinement, and creation of publication materials were performed using SHELXTL[4]. ORTEP diagrams were created using ORTEP-3.[5]

Preparation of $[Fe^{II}(N(TMS)_2)_2(PCy_3)]$, (**1**):
PCy_3 (1.00 g, 3.57 mmol) and $FeCl_2$ (452 mg, 3.57 mmol) were added to a 20 mL vial followed by THF (ca. 10 mL) and the mixture was stirred overnight. The resulting off-white suspension was cooled to ca. -25°C and $KN(TMS)_2$ (1.423 g, 7.13 mmol) was added in portions with stirring to give a dark mixture. This mixture was filtered through Celite to give a dark solution that was reduced to dryness in vacuo. The residue was taken up in pentane and filtered through Celite. The filtrate was then concentrated until solid began to form, followed by cooling to ca. -25 C giving very lightly colored solid and a dark solution. The solution was removed and the remaining solid redissolved in pentane. This procedure was repeated until the resulting pentane solution was a very slight green color. Subsequently, the very slightly green/blue tinted solid was collected and washed with cold pentane (990 mg, 42 %). Anal. Elemental analysis, % found (calc'd): C: 54.79 (54.84), H: 10.48 (10.58), N: 4.06 (4.26).

Preparation of $([Fe^{II}(N(TMS)_2)_2(depe)]$, (**2**):
Anhydrous $FeBr_2$ (180 mg, 0.84 mmol) and $KN(TMS)_2$ (333 mg, 1.70 mmol) were dissolved separately in THF (15 mL), cooled to -25°C, added together dropwise, allowed to warm to ambient temperature and stirred for 15 hours. To this suspension was added bis(diethylphosphino)ethane (depe) (172 mg, 0.83 mmol) with a further 24 hours of stirring. The olive-brown mixture was filtered through Celite and the solvent was removed *in vacuo*. The resulting brownish solid was extracted with hexanes, the volume was reduced and the sample placed in a -25°C freezer until yellowish-brown crystals were obtained (58 mg, 12% yield). Elemental analysis, % found (calc'd): C 45.39 (45.33), H 10.22 (10.38%,) N 4.68 (4.81).

Magnetic Measurements:

Sample preparation was carried out in inert atmospheric glove box. The magnetic susceptibility measurements were obtained using a Quantum Design SQUID magnetometer MPMS-XL7 operating between 1.8 and 300 K for dc-applied fields ranging from -7 to 7 T. Dc analyses were performed on polycrystalline samples of 20 and 17 mg for **1** and **2,** respectively, restrained in a polyethylene membrane and under a field ranging from 0 to 7 T between 1.8 and 300 K. Ac susceptibility measurements were carried out under an oscillating ac field of 3 Oe and ac frequencies ranging from 1 to 1500 Hz. The magnetization data were collected at 100 K to check for ferromagnetic impurities that were absent in all samples. A diamagnetic correction was applied for the sample holder and the sample.

Computational details:

Density functional theory (DFT) calculations were carried out with the Gaussian 09 software (revision A.02).[6] Geometry optimization calculations were carried out for the complexes constructed using the crystal structures as starting points using the spin-unrestricted molecular orbital formalism. The triple-zeta TZVP basis set[7] for all atoms was used. Unless notified otherwise, the calculations employed the PBE exchange-correlation functional (PBE exchange and PBE correlation).[8] Calculations were also repeated using the hybrid B3LYP functional.[9] The wavefunction stability checks were performed to make sure that the calculated wavefunction corresponds to the electronic ground state (the *stable* keyword in Gaussian). The energies of 20 lowest quintet excited states were calculated using time-dependent DFT calculations[10] utilizing the optimized ground state geometries. Atomic spin densities and charges were evaluated by using the natural population analysis (NPA)[11] as implemented in the Gaussian 09 program. Mayer bond orders[12] and atomic compositions[13] of canonical molecular orbitals were calculated using the AOMix software.[14]

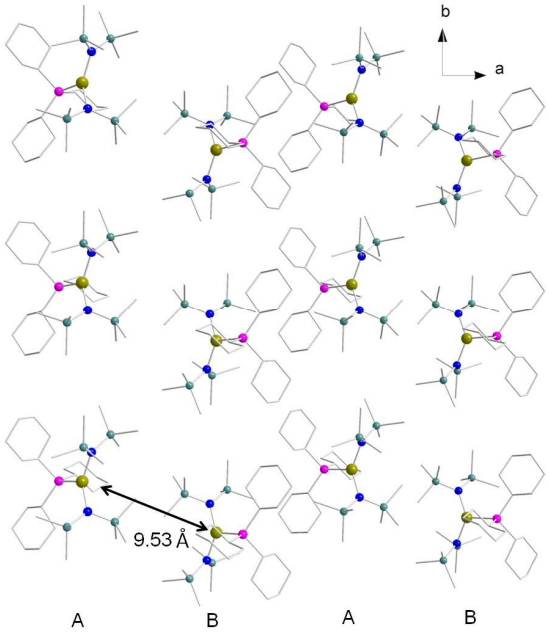

Figure S1. Packing arrangement of **1** along the crystallographic *c* axis.

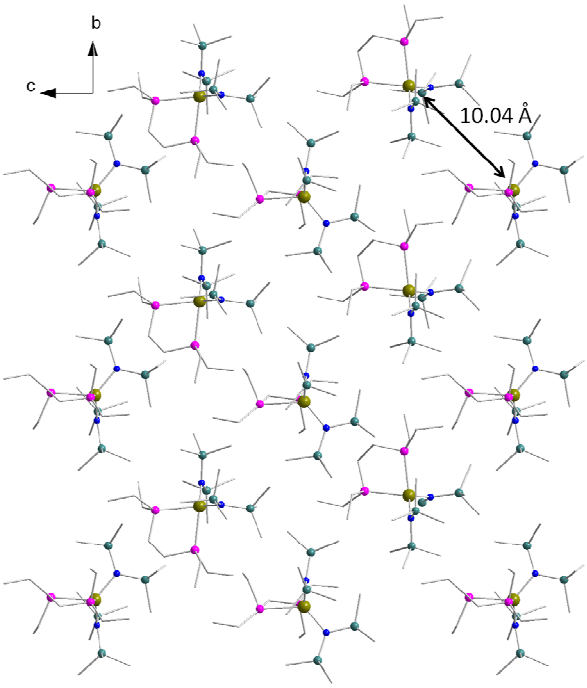

Figure S2. Packing arrangement of **2** along the crystallographic *a* axis.

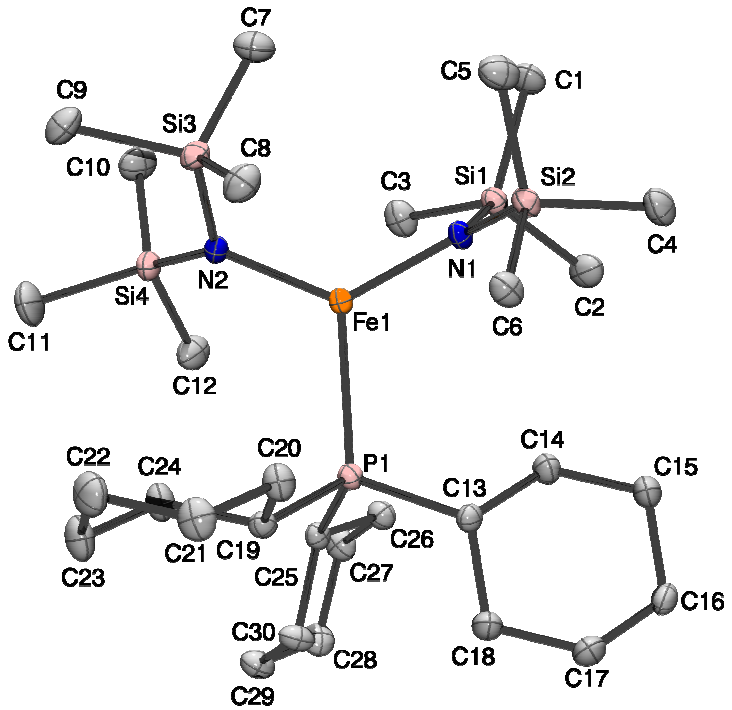

Figure S3. Fully labeled ORTEP diagram of **1**. Thermal ellipsoids at 50 % probability. Hydrogen atoms are omitted for clarity.

Table S1. Crystal data and structure refinement for **1.**

Identification code	apx1282	
Empirical formula	C_{30} H_{69} Fe N_2 P Si_4	
Formula weight	657.05	
Temperature	120(1) K	
Wavelength	0.71073 Å	
Crystal system	Monoclinic	
Space group	P 2_1/n	
Unit cell dimensions	a = 12.0279(9) Å	α = 90°.
	b = 15.7960(12) Å	β = 90.3290(10)°.
	c = 20.3153(16) Å	γ = 90°.
Volume	3859.7(5) $Å^3$	
Z	4	
Density (calculated)	1.131 Mg/m^3	
Absorption coefficient	0.577 mm^{-1}	
F(000)	1440	
Crystal size	0.30 x 0.20 x 0.14 mm^3	
Theta range for data collection	1.97 to 28.36°.	
Index ranges	-15<=h<=15, -20<=k<=20, -25<=l<=26	
Reflections collected	43164	
Independent reflections	9060 [R(int) = 0.0687]	
Completeness to theta = 25.50°	99.7 %	
Absorption correction	Semi-empirical from equivalents	
Max. and min. transmission	0.9236 and 0.8459	
Refinement method	Full-matrix least-squares on F^2	
Data / restraints / parameters	9060 / 0 / 355	
Goodness-of-fit on F^2	1.124	
Final R indices [I>2sigma(I)]	R_1 = 0.0388, wR_2 = 0.0880	
R indices (all data)	R_1 = 0.0606, wR_2 = 0.0960	
Largest diff. peak and hole	0.405 and -0.309 e.$Å^{-3}$	

Table S2. Atomic coordinates (x 10^4) and equivalent isotropic displacement parameters (Å^{2}x 10^3) for **1**. U(eq) is defined as one third of the trace of the orthogonalized U^{ij} tensor.

	x	y	z	U(eq)
Fe(1)	-289(1)	8436(1)	2415(1)	13(1)
P(1)	1572(1)	7863(1)	2072(1)	14(1)
Si(1)	-423(1)	9767(1)	3505(1)	17(1)
Si(2)	-641(1)	7980(1)	3974(1)	17(1)
Si(3)	-2619(1)	8023(1)	1982(1)	18(1)
Si(4)	-1440(1)	9176(1)	1056(1)	18(1)
N(1)	-425(1)	8696(1)	3350(1)	15(1)
N(2)	-1422(1)	8513(1)	1728(1)	15(1)
C(1)	-1599(2)	10118(1)	4039(1)	25(1)
C(2)	916(2)	10160(1)	3871(1)	26(1)
C(3)	-551(2)	10357(1)	2716(1)	26(1)
C(4)	67(2)	8305(1)	4756(1)	26(1)
C(5)	-2153(2)	7834(1)	4175(1)	27(1)
C(6)	-50(2)	6913(1)	3775(1)	21(1)
C(7)	-3433(2)	8716(1)	2548(1)	27(1)
C(8)	-2266(2)	7014(1)	2421(1)	26(1)
C(9)	-3577(2)	7703(1)	1294(1)	27(1)
C(10)	-2546(2)	10007(1)	1110(1)	29(1)
C(11)	-1675(2)	8599(2)	264(1)	34(1)
C(12)	-100(2)	9754(1)	944(1)	27(1)
C(13)	2465(2)	7583(1)	2787(1)	15(1)
C(14)	2484(2)	8290(1)	3303(1)	20(1)
C(15)	3082(2)	8010(1)	3933(1)	21(1)
C(16)	4255(2)	7706(1)	3788(1)	21(1)
C(17)	4237(2)	7005(1)	3278(1)	24(1)
C(18)	3645(2)	7281(1)	2645(1)	21(1)
C(19)	1423(2)	6874(1)	1588(1)	15(1)
C(20)	829(2)	6186(1)	1984(1)	20(1)
C(21)	640(2)	5386(1)	1579(1)	25(1)
C(22)	2(2)	5576(1)	945(1)	29(1)
C(23)	607(2)	6243(1)	546(1)	27(1)
C(24)	786(2)	7050(1)	946(1)	22(1)

C(25)	2338(2)	8573(1)	1508(1)	15(1)
C(26)	2658(2)	9424(1)	1822(1)	19(1)
C(27)	3035(2)	10046(1)	1294(1)	22(1)
C(28)	3993(2)	9698(1)	893(1)	24(1)
C(29)	3693(2)	8839(1)	598(1)	23(1)
C(30)	3323(2)	8214(1)	1124(1)	21(1)

Table S3. Bond lengths [Å] and angles [°] for **1**.

Fe(1)-N(1)	1.9496(16)
Fe(1)-N(2)	1.9503(16)
Fe(1)-P(1)	2.5167(6)
P(1)-C(25)	1.8524(19)
P(1)-C(13)	1.8542(19)
P(1)-C(19)	1.8547(19)
Si(1)-N(1)	1.7210(17)
Si(1)-C(3)	1.861(2)
Si(1)-C(1)	1.872(2)
Si(1)-C(2)	1.875(2)
Si(2)-N(1)	1.7199(16)
Si(2)-C(4)	1.870(2)
Si(2)-C(6)	1.873(2)
Si(2)-C(5)	1.880(2)
Si(3)-N(2)	1.7168(17)
Si(3)-C(7)	1.869(2)
Si(3)-C(8)	1.874(2)
Si(3)-C(9)	1.875(2)
Si(4)-N(2)	1.7198(16)
Si(4)-C(12)	1.868(2)
Si(4)-C(11)	1.871(2)
Si(4)-C(10)	1.873(2)
C(13)-C(18)	1.527(3)
C(13)-C(14)	1.533(3)
C(14)-C(15)	1.529(3)

C(15)-C(16)	1.520(3)
C(16)-C(17)	1.518(3)
C(17)-C(18)	1.529(3)
C(19)-C(20)	1.531(3)
C(19)-C(24)	1.534(3)
C(20)-C(21)	1.525(3)
C(21)-C(22)	1.525(3)
C(22)-C(23)	1.517(3)
C(23)-C(24)	1.527(3)
C(25)-C(30)	1.532(3)
C(25)-C(26)	1.536(3)
C(26)-C(27)	1.524(3)
C(27)-C(28)	1.518(3)
C(28)-C(29)	1.527(3)
C(29)-C(30)	1.522(3)

N(1)-Fe(1)-N(2)	128.46(7)
N(1)-Fe(1)-P(1)	115.16(5)
N(2)-Fe(1)-P(1)	116.31(5)
C(25)-P(1)-C(13)	109.92(9)
C(25)-P(1)-C(19)	103.19(9)
C(13)-P(1)-C(19)	105.59(9)
C(25)-P(1)-Fe(1)	113.53(6)
C(13)-P(1)-Fe(1)	112.42(6)
C(19)-P(1)-Fe(1)	111.51(6)
N(1)-Si(1)-C(3)	109.52(9)
N(1)-Si(1)-C(1)	113.41(9)
C(3)-Si(1)-C(1)	106.97(10)
N(1)-Si(1)-C(2)	113.53(9)
C(3)-Si(1)-C(2)	104.00(10)
C(1)-Si(1)-C(2)	108.79(10)
N(1)-Si(2)-C(4)	112.07(9)
N(1)-Si(2)-C(6)	111.92(9)
C(4)-Si(2)-C(6)	104.99(10)
N(1)-Si(2)-C(5)	113.03(9)
C(4)-Si(2)-C(5)	106.59(10)
C(6)-Si(2)-C(5)	107.76(10)

N(2)-Si(3)-C(7)	111.35(9)
N(2)-Si(3)-C(8)	109.78(9)
C(7)-Si(3)-C(8)	108.88(10)
N(2)-Si(3)-C(9)	114.17(9)
C(7)-Si(3)-C(9)	107.13(10)
C(8)-Si(3)-C(9)	105.24(10)
N(2)-Si(4)-C(12)	112.84(9)
N(2)-Si(4)-C(11)	112.75(10)
C(12)-Si(4)-C(11)	105.02(11)
N(2)-Si(4)-C(10)	112.74(9)
C(12)-Si(4)-C(10)	106.17(10)
C(11)-Si(4)-C(10)	106.73(11)
Si(2)-N(1)-Si(1)	120.74(9)
Si(2)-N(1)-Fe(1)	126.41(9)
Si(1)-N(1)-Fe(1)	112.66(8)
Si(3)-N(2)-Si(4)	120.46(9)
Si(3)-N(2)-Fe(1)	109.90(8)
Si(4)-N(2)-Fe(1)	127.66(9)
C(18)-C(13)-C(14)	110.32(16)
C(18)-C(13)-P(1)	117.50(13)
C(14)-C(13)-P(1)	111.61(13)
C(15)-C(14)-C(13)	111.52(16)
C(16)-C(15)-C(14)	111.22(16)
C(17)-C(16)-C(15)	110.70(17)
C(16)-C(17)-C(18)	111.81(17)
C(13)-C(18)-C(17)	111.01(17)
C(20)-C(19)-C(24)	110.06(16)
C(20)-C(19)-P(1)	111.22(13)
C(24)-C(19)-P(1)	110.18(13)
C(21)-C(20)-C(19)	111.86(16)
C(22)-C(21)-C(20)	111.47(17)
C(23)-C(22)-C(21)	110.32(18)
C(22)-C(23)-C(24)	111.25(18)
C(23)-C(24)-C(19)	111.66(17)
C(30)-C(25)-C(26)	110.00(16)
C(30)-C(25)-P(1)	118.69(13)
C(26)-C(25)-P(1)	113.47(13)

C(27)-C(26)-C(25)	110.35(16)
C(28)-C(27)-C(26)	111.92(17)
C(27)-C(28)-C(29)	110.70(17)
C(30)-C(29)-C(28)	111.74(17)
C(29)-C(30)-C(25)	110.34(16)

Table S4. Anisotropic displacement parameters ($Å^2 x 10^3$) for **1**. The anisotropic displacement factor exponent takes the form: $-2\pi^2[h^2 a^{*2} U^{11} + ... + 2 h k a^* b^* U^{12}]$

	U^{11}	U^{22}	U^{33}	U^{23}	U^{13}	U^{12}
Fe(1)	15(1)	14(1)	11(1)	0(1)	0(1)	0(1)
P(1)	15(1)	13(1)	13(1)	0(1)	0(1)	1(1)
Si(1)	19(1)	15(1)	15(1)	-1(1)	0(1)	2(1)
Si(2)	21(1)	17(1)	13(1)	1(1)	2(1)	3(1)
Si(3)	14(1)	20(1)	21(1)	-1(1)	-1(1)	-2(1)
Si(4)	19(1)	23(1)	14(1)	1(1)	-2(1)	1(1)
N(1)	19(1)	15(1)	12(1)	1(1)	0(1)	3(1)
N(2)	14(1)	18(1)	13(1)	0(1)	-2(1)	-1(1)
C(1)	26(1)	24(1)	25(1)	-6(1)	4(1)	6(1)
C(2)	26(1)	22(1)	30(1)	-7(1)	-1(1)	0(1)
C(3)	36(1)	18(1)	23(1)	-1(1)	0(1)	1(1)
C(4)	34(1)	26(1)	17(1)	2(1)	1(1)	5(1)
C(5)	28(1)	28(1)	25(1)	6(1)	7(1)	3(1)
C(6)	26(1)	17(1)	19(1)	2(1)	2(1)	2(1)
C(7)	23(1)	28(1)	31(1)	0(1)	8(1)	0(1)
C(8)	23(1)	24(1)	31(1)	4(1)	-3(1)	-5(1)
C(9)	20(1)	27(1)	34(1)	0(1)	-7(1)	-5(1)
C(10)	27(1)	30(1)	31(1)	8(1)	-1(1)	5(1)
C(11)	44(2)	43(2)	15(1)	0(1)	-4(1)	-1(1)
C(12)	25(1)	34(1)	22(1)	10(1)	-1(1)	-2(1)
C(13)	16(1)	16(1)	13(1)	2(1)	-1(1)	1(1)

C(14)	21(1)	21(1)	17(1)	-3(1)	-2(1)	3(1)
C(15)	21(1)	27(1)	16(1)	-2(1)	-1(1)	3(1)
C(16)	16(1)	29(1)	16(1)	3(1)	-3(1)	-1(1)
C(17)	19(1)	29(1)	23(1)	-1(1)	-3(1)	7(1)
C(18)	19(1)	25(1)	20(1)	-4(1)	-1(1)	5(1)
C(19)	15(1)	15(1)	16(1)	-1(1)	1(1)	2(1)
C(20)	25(1)	17(1)	19(1)	1(1)	-1(1)	-3(1)
C(21)	30(1)	17(1)	26(1)	1(1)	0(1)	-6(1)
C(22)	33(1)	26(1)	29(1)	-9(1)	-4(1)	-7(1)
C(23)	38(1)	23(1)	20(1)	-4(1)	-4(1)	-4(1)
C(24)	29(1)	19(1)	17(1)	-1(1)	-3(1)	-1(1)
C(25)	18(1)	14(1)	14(1)	1(1)	0(1)	1(1)
C(26)	20(1)	17(1)	19(1)	-1(1)	1(1)	-1(1)
C(27)	26(1)	17(1)	23(1)	-2(1)	2(1)	-4(1)
C(28)	25(1)	27(1)	21(1)	4(1)	4(1)	-6(1)
C(29)	25(1)	21(1)	21(1)	1(1)	6(1)	2(1)
C(30)	22(1)	18(1)	22(1)	3(1)	8(1)	4(1)

Table S5. Hydrogen coordinates (x 10^4) and isotropic displacement parameters (Å^{2}x 10^3) for **1**.

	x	y	z	U(eq)
H(1A)	-2293	9971	3833	38
H(1B)	-1563	10720	4099	38
H(1C)	-1545	9843	4460	38
H(2A)	1049	9882	4284	39
H(2B)	867	10760	3940	39
H(2C)	1515	10040	3575	39
H(3A)	64	10217	2437	39
H(3B)	-548	10954	2803	39
H(3C)	-1234	10204	2500	39
H(4A)	855	8334	4686	38

H(4B)	-87	7897	5093	38
H(4C)	-203	8850	4889	38
H(5A)	-2459	8362	4320	41
H(5B)	-2225	7420	4518	41
H(5C)	-2546	7644	3790	41
H(6A)	-179	6789	3318	31
H(6B)	-404	6491	4041	31
H(6C)	734	6914	3863	31
H(7A)	-2980	8868	2920	41
H(7B)	-4080	8417	2696	41
H(7C)	-3658	9219	2318	41
H(8A)	-2020	6600	2108	39
H(8B)	-2912	6806	2644	39
H(8C)	-1684	7119	2736	39
H(9A)	-3859	8201	1079	41
H(9B)	-4185	7381	1468	41
H(9C)	-3177	7364	983	41
H(10A)	-3261	9740	1143	44
H(10B)	-2528	10354	722	44
H(10C)	-2416	10353	1491	44
H(11A)	-1218	8101	254	51
H(11B)	-1484	8961	-98	51
H(11C)	-2443	8439	228	51
H(12A)	228	9869	1366	41
H(12B)	-237	10278	718	41
H(12C)	399	9413	689	41
H(13)	2095	7103	2999	18
H(14A)	2857	8782	3123	23
H(14B)	1727	8452	3408	23
H(15A)	3115	8481	4239	25
H(15B)	2665	7557	4139	25
H(16A)	4696	8175	3628	25
H(16B)	4597	7498	4191	25
H(17A)	3861	6514	3458	28
H(17B)	4994	6841	3176	28
H(18A)	4062	7735	2440	25
H(18B)	3618	6809	2339	25

H(19)	2167	6668	1476	18
H(20A)	1270	6048	2370	24
H(20B)	117	6402	2132	24
H(21A)	1352	5135	1471	29
H(21B)	226	4980	1838	29
H(22A)	-71	5062	687	35
H(22B)	-738	5776	1050	35
H(23A)	176	6374	153	32
H(23B)	1321	6022	408	32
H(24A)	70	7299	1048	26
H(24B)	1199	7455	684	26
H(25)	1791	8722	1168	18
H(26A)	2024	9656	2053	22
H(26B)	3254	9338	2138	22
H(27A)	2415	10170	1002	27
H(27B)	3263	10571	1502	27
H(28A)	4645	9639	1173	29
H(28B)	4171	10091	543	29
H(29A)	3099	8911	278	27
H(29B)	4333	8611	371	27
H(30A)	3936	8102	1424	25
H(30B)	3109	7684	918	25

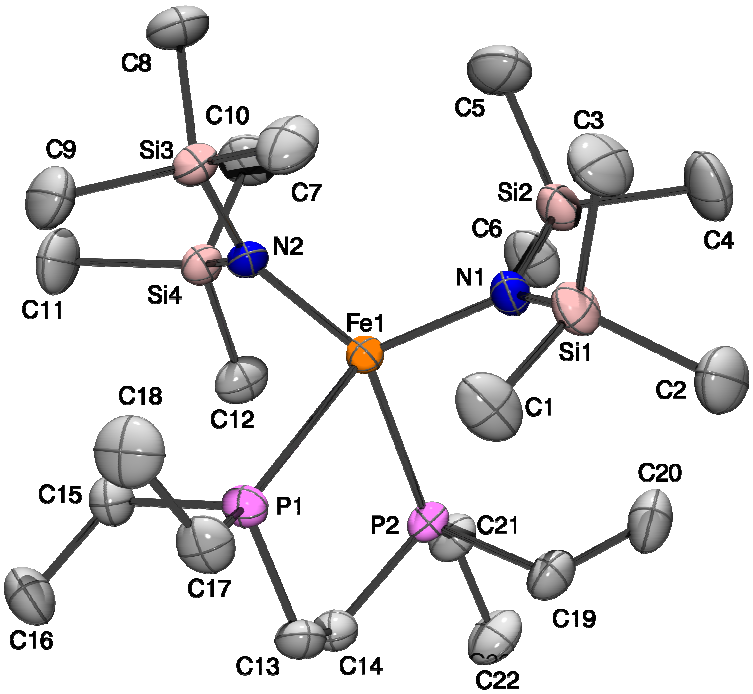

Figure S4. ORTEP diagram of **2** with hydrogen atoms omitted for clarity. Thermal ellipsoids are at 50% probability.

Table S6. Crystal data and structure refinement for **2**.

Identification code	tb018	
Empirical formula	$C_{22}H_{60}FeN_2P_2Si_4$	
Formula weight	582.87	
Temperature	200(2) K	
Wavelength	0.71073 Å	
Crystal system, space group	Tetragonal, $P4_1$	
Unit cell dimensions	a = 11.9184(3) Å	α = 90°
	b = 11.9184(3) Å	β = 90°
	c = 24.2844(8) Å	γ = 90°
Volume	3449.56(17) $Å^3$	
Z, Calculated density	4, 1.122 Mg/m^3	
Absorption coefficient	0.682 mm^-1	
F(000)	1272	
Crystal size	0.19 x 0.17 x 0.06 mm	
Theta range for data collection	1.90 to 28.28 deg.	
Limiting indices	-15<=h<=15, -14<=k<=15, -32<=l<=32	
Reflections collected / unique	46964 / 8407 [R(int) = 0.0330]	
Completeness to theta = 28.28°	99.1 %	
Absorption correction	Semi-empirical from equivalents	
Max. and min. transmission	0.9602 and 0.8814	
Refinement method	Full-matrix least-squares on F^2	
Data / restraints / parameters	8407 / 1 / 280	
Goodness-of-fit on F^2	1.042	
Final R indices [I>2sigma(I)]	R_1 = 0.0286, wR_2 = 0.0591	
R indices (all data)	R_1 = 0.0370, wR_2 = 0.0612	
Absolute structure parameter	0.000(8)	
Largest diff. peak and hole	0.263 and -0.173 e.A^-3	

Table S7. Atomic coordinates (x 10^4) and equivalent isotropic displacement parameters (A^2 x 10^3) for **2**. U(eq) is defined as one third of the trace of the orthogonalized Uij tensor.

	x	y	z	U(eq)
Fe(1)	9745(1)	4841(1)	992(1)	23(1)
N(1)	10856(1)	6090(1)	949(1)	30(1)
N(2)	9816(1)	3553(1)	472(1)	28(1)
Si(1)	10497(1)	7465(1)	831(1)	37(1)
Si(2)	12227(1)	5649(1)	928(1)	37(1)
Si(3)	9627(1)	3861(1)	-213(1)	35(1)
Si(4)	10077(1)	2197(1)	671(1)	32(1)
P(1)	7581(1)	4943(1)	1104(1)	28(1)
P(2)	9530(1)	4718(1)	2051(1)	27(1)
C(1)	8935(2)	7647(2)	806(1)	51(1)
C(2)	10949(2)	8487(2)	1380(1)	55(1)
C(3)	11066(2)	8038(2)	164(1)	58(1)
C(4)	13268(2)	6766(2)	1126(1)	62(1)
C(5)	12685(2)	5141(3)	232(1)	60(1)
C(6)	12494(2)	4461(2)	1419(1)	53(1)
C(7)	9730(2)	5413(2)	-345(1)	52(1)
C(8)	10663(2)	3146(2)	-685(1)	57(1)
C(9)	8222(2)	3429(2)	-497(1)	53(1)
C(10)	11545(2)	1722(2)	511(1)	55(1)
C(11)	9116(2)	1131(2)	342(1)	55(1)
C(12)	9925(2)	1983(2)	1430(1)	42(1)
C(13)	7267(2)	5136(2)	1840(1)	36(1)
C(14)	8043(2)	4431(2)	2204(1)	34(1)
C(15)	7025(2)	3528(2)	968(1)	35(1)
C(16)	5787(2)	3318(2)	1099(1)	50(1)
C(17)	6510(2)	5877(2)	806(1)	40(1)
C(18)	6364(2)	5782(2)	187(1)	55(1)
C(19)	9686(2)	6134(2)	2343(1)	39(1)
C(20)	10899(2)	6465(2)	2454(1)	53(1)
C(21)	10259(2)	3832(2)	2557(1)	38(1)

C(22)	9997(2)	4047(2)	3164(1)	51(1)

Table S8. Bond lengths [Å] and angles [°] for **2**.

Fe(1)-N(2)	1.9886(15)
Fe(1)-N(1)	1.9949(15)
Fe(1)-P(2)	2.5878(5)
Fe(1)-P(1)	2.5965(5)
N(1)-Si(1)	1.7178(16)
N(1)-Si(2)	1.7176(16)
N(2)-Si(3)	1.7192(16)
N(2)-Si(4)	1.7161(17)
Si(1)-C(1)	1.875(2)
Si(1)-C(3)	1.883(2)
Si(1)-C(2)	1.885(2)
Si(2)-C(5)	1.876(3)
Si(2)-C(6)	1.879(3)
Si(2)-C(4)	1.883(2)
Si(3)-C(7)	1.882(2)
Si(3)-C(9)	1.883(2)
Si(3)-C(8)	1.888(2)
Si(4)-C(12)	1.870(2)
Si(4)-C(10)	1.880(2)
Si(4)-C(11)	1.888(2)
P(1)-C(13)	1.839(2)
P(1)-C(17)	1.842(2)
P(1)-C(15)	1.8421(19)
P(2)-C(19)	1.840(2)
P(2)-C(21)	1.838(2)
P(2)-C(14)	1.843(2)
C(13)-C(14)	1.532(3)
C(15)-C(16)	1.530(3)
C(17)-C(18)	1.518(3)
C(19)-C(20)	1.523(3)
C(21)-C(22)	1.529(3)
N(2)-Fe(1)-N(1)	120.93(6)
N(2)-Fe(1)-P(2)	126.22(5)

N(1)-Fe(1)-P(2)	99.24(5)
N(2)-Fe(1)-P(1)	98.33(5)
N(1)-Fe(1)-P(1)	129.06(5)
P(2)-Fe(1)-P(1)	78.454(17)
Si(1)-N(1)-Si(2)	121.60(9)
Si(1)-N(1)-Fe(1)	123.73(8)
Si(2)-N(1)-Fe(1)	113.88(8)
Si(3)-N(2)-Si(4)	119.81(9)
Si(3)-N(2)-Fe(1)	116.38(9)
Si(4)-N(2)-Fe(1)	123.79(9)
N(1)-Si(1)-C(1)	111.29(9)
N(1)-Si(1)-C(3)	113.55(11)
C(1)-Si(1)-C(3)	106.69(12)
N(1)-Si(1)-C(2)	115.31(10)
C(1)-Si(1)-C(2)	103.43(12)
C(3)-Si(1)-C(2)	105.71(12)
N(1)-Si(2)-C(5)	113.70(11)
N(1)-Si(2)-C(6)	111.87(9)
C(5)-Si(2)-C(6)	106.28(13)
N(1)-Si(2)-C(4)	113.77(10)
C(5)-Si(2)-C(4)	105.46(13)
C(6)-Si(2)-C(4)	105.03(13)
N(2)-Si(3)-C(7)	111.44(9)
N(2)-Si(3)-C(9)	114.39(10)
C(7)-Si(3)-C(9)	105.36(11)
N(2)-Si(3)-C(8)	113.93(11)
C(7)-Si(3)-C(8)	107.36(12)
C(9)-Si(3)-C(8)	103.63(12)
N(2)-Si(4)-C(12)	112.85(8)
N(2)-Si(4)-C(10)	113.25(10)
C(12)-Si(4)-C(10)	104.64(12)
N(2)-Si(4)-C(11)	113.87(10)
C(12)-Si(4)-C(11)	105.46(12)
C(10)-Si(4)-C(11)	105.96(12)
C(13)-P(1)-C(17)	99.50(10)
C(13)-P(1)-C(15)	102.50(10)
C(17)-P(1)-C(15)	103.52(10)

C(13)-P(1)-Fe(1)	108.05(7)
C(17)-P(1)-Fe(1)	132.46(7)
C(15)-P(1)-Fe(1)	107.19(6)
C(19)-P(2)-C(21)	102.78(10)
C(19)-P(2)-C(14)	100.90(10)
C(21)-P(2)-C(14)	102.26(10)
C(19)-P(2)-Fe(1)	108.72(7)
C(21)-P(2)-Fe(1)	130.54(7)
C(14)-P(2)-Fe(1)	107.87(6)
C(14)-C(13)-P(1)	111.70(13)
C(13)-C(14)-P(2)	111.18(14)
C(16)-C(15)-P(1)	117.34(15)
C(18)-C(17)-P(1)	115.06(15)
C(20)-C(19)-P(2)	113.69(15)
C(22)-C(21)-P(2)	116.89(16)

Table S9. Anisotropic displacement parameters (A^2 x 10^3) for **2**. The anisotropic displacement factor exponent takes the form: -2 pi^2 [h^2 a^{*2} U11 + ... + 2 h k a* b* U12]

	U11	U22	U33	U23	U13	U12
Fe(1)	23(1)	22(1)	25(1)	-2(1)	1(1)	0(1)
N(1)	27(1)	28(1)	35(1)	-2(1)	1(1)	-4(1)
N(2)	27(1)	30(1)	26(1)	-6(1)	4(1)	0(1)
Si(1)	35(1)	27(1)	48(1)	5(1)	4(1)	-4(1)
Si(2)	24(1)	40(1)	48(1)	-6(1)	3(1)	-2(1)
Si(3)	37(1)	44(1)	25(1)	-6(1)	2(1)	-3(1)
Si(4)	31(1)	27(1)	36(1)	-8(1)	3(1)	2(1)
P(1)	23(1)	30(1)	30(1)	1(1)	0(1)	4(1)
P(2)	31(1)	26(1)	23(1)	-2(1)	-1(1)	2(1)
C(1)	43(1)	33(1)	76(2)	12(1)	3(1)	8(1)
C(2)	65(2)	32(1)	68(2)	-6(1)	3(1)	-6(1)
C(3)	73(2)	43(1)	60(2)	15(1)	12(1)	-13(1)
C(4)	31(1)	57(2)	97(2)	-10(2)	-6(1)	-10(1)
C(5)	41(1)	80(2)	59(2)	-13(1)	12(1)	6(1)
C(6)	30(1)	54(2)	76(2)	4(1)	-2(1)	8(1)
C(7)	74(2)	51(2)	30(1)	8(1)	-3(1)	-4(1)
C(8)	59(2)	73(2)	39(1)	-17(1)	15(1)	0(1)
C(9)	51(1)	66(2)	40(1)	-8(1)	-14(1)	-5(1)
C(10)	44(1)	49(1)	70(2)	-7(1)	11(1)	17(1)
C(11)	68(2)	32(1)	66(2)	-11(1)	-12(1)	-10(1)
C(12)	56(1)	30(1)	40(1)	1(1)	3(1)	8(1)
C(13)	31(1)	41(1)	34(1)	-6(1)	8(1)	4(1)
C(14)	37(1)	37(1)	27(1)	-1(1)	4(1)	-3(1)
C(15)	34(1)	33(1)	37(1)	0(1)	-2(1)	-2(1)
C(16)	35(1)	55(1)	59(2)	1(1)	0(1)	-11(1)
C(17)	32(1)	37(1)	50(1)	3(1)	-4(1)	11(1)
C(18)	53(2)	59(2)	52(2)	12(1)	-14(1)	13(1)
C(19)	51(1)	30(1)	37(1)	-7(1)	0(1)	2(1)
C(20)	66(2)	43(1)	50(1)	-9(1)	-11(1)	-12(1)
C(21)	46(1)	39(1)	29(1)	1(1)	-8(1)	6(1)
C(22)	76(2)	50(1)	27(1)	0(1)	-10(1)	4(1)

Table S10. Hydrogen coordinates (x 10^4) and isotropic displacement parameters (A^2 x 10^3) for **2**.

	x	y	z	U(eq)
H(1A)	8619	7143	527	76
H(1B)	8756	8426	710	76
H(1C)	8613	7467	1166	76
H(2A)	10683	8227	1740	83
H(2B)	10630	9228	1302	83
H(2C)	11770	8538	1385	83
H(3A)	10853	7540	-139	88
H(3B)	11885	8085	186	88
H(3C)	10755	8788	99	88
H(4A)	13071	7071	1488	93
H(4B)	13253	7369	851	93
H(4C)	14022	6440	1140	93
H(5A)	12176	4548	106	90
H(5B)	13449	4843	256	90
H(5C)	12668	5766	-30	90
H(6A)	11983	3840	1336	80
H(6B)	12366	4719	1797	80
H(6C)	13271	4206	1381	80
H(7A)	10448	5694	-204	78
H(7B)	9113	5799	-156	78
H(7C)	9682	5556	-741	78
H(8A)	11428	3323	-566	85
H(8B)	10550	3410	-1063	85
H(8C)	10548	2332	-670	85
H(9A)	7623	3765	-275	79
H(9B)	8156	2609	-485	79
H(9C)	8155	3686	-879	79
H(10A)	12083	2253	670	82
H(10B)	11649	1691	111	82
H(10C)	11670	975	669	82
H(11A)	8334	1335	416	83
H(11B)	9270	387	497	83

H(11C)	9246	1117	-56	83
H(12A)	10409	2515	1626	63
H(12B)	10145	1214	1525	63
H(12C)	9142	2107	1537	63
H(13A)	7354	5939	1937	43
H(13B)	6478	4921	1911	43
H(14A)	7885	3625	2144	40
H(14B)	7891	4602	2596	40
H(15A)	7147	3358	574	41
H(15B)	7477	2985	1183	41
H(16A)	5596	2539	1010	75
H(16B)	5320	3825	879	75
H(16C)	5651	3455	1491	75
H(17A)	5781	5713	984	48
H(17B)	6710	6662	897	48
H(18A)	5779	6304	65	82
H(18B)	6147	5013	92	82
H(18C)	7073	5969	4	82
H(19A)	9351	6683	2085	47
H(19B)	9260	6173	2692	47
H(20A)	10921	7224	2609	79
H(20B)	11323	6448	2108	79
H(20C)	11232	5936	2716	79
H(21A)	10078	3039	2474	45
H(21B)	11076	3927	2502	45
H(22A)	10435	3530	3393	76
H(22B)	9195	3925	3231	76
H(22C)	10193	4822	3258	76

Table S11. Torsion angles [°] for **2**.

N(2)-Fe(1)-N(1)-Si(1)	119.91(10)
P(2)-Fe(1)-N(1)-Si(1)	-97.40(10)
P(1)-Fe(1)-N(1)-Si(1)	-14.82(14)
N(2)-Fe(1)-N(1)-Si(2)	-50.06(12)
P(2)-Fe(1)-N(1)-Si(2)	92.62(9)
P(1)-Fe(1)-N(1)-Si(2)	175.20(5)
N(1)-Fe(1)-N(2)-Si(3)	-62.77(11)
P(2)-Fe(1)-N(2)-Si(3)	165.10(6)
P(1)-Fe(1)-N(2)-Si(3)	83.35(8)
N(1)-Fe(1)-N(2)-Si(4)	115.89(10)
P(2)-Fe(1)-N(2)-Si(4)	-16.24(13)
P(1)-Fe(1)-N(2)-Si(4)	-97.99(9)
Si(2)-N(1)-Si(1)-C(1)	173.73(12)
Fe(1)-N(1)-Si(1)-C(1)	4.50(15)
Si(2)-N(1)-Si(1)-C(3)	53.32(16)
Fe(1)-N(1)-Si(1)-C(3)	-115.91(13)
Si(2)-N(1)-Si(1)-C(2)	-68.88(15)
Fe(1)-N(1)-Si(1)-C(2)	121.89(12)
Si(1)-N(1)-Si(2)-C(5)	-91.44(15)
Fe(1)-N(1)-Si(2)-C(5)	78.77(14)
Si(1)-N(1)-Si(2)-C(6)	148.16(13)
Fe(1)-N(1)-Si(2)-C(6)	-41.63(14)
Si(1)-N(1)-Si(2)-C(4)	29.33(17)
Fe(1)-N(1)-Si(2)-C(4)	-160.46(12)
Si(4)-N(2)-Si(3)-C(7)	-165.17(12)
Fe(1)-N(2)-Si(3)-C(7)	13.55(14)
Si(4)-N(2)-Si(3)-C(9)	75.46(14)
Fe(1)-N(2)-Si(3)-C(9)	-105.83(12)
Si(4)-N(2)-Si(3)-C(8)	-43.51(15)
Fe(1)-N(2)-Si(3)-C(8)	135.21(11)
Si(3)-N(2)-Si(4)-C(12)	-166.63(11)
Fe(1)-N(2)-Si(4)-C(12)	14.76(14)
Si(3)-N(2)-Si(4)-C(10)	74.72(14)
Fe(1)-N(2)-Si(4)-C(10)	-103.90(13)
Si(3)-N(2)-Si(4)-C(11)	-46.44(15)

Fe(1)-N(2)-Si(4)-C(11)	134.95(12)
N(2)-Fe(1)-P(1)-C(13)	136.01(9)
N(1)-Fe(1)-P(1)-C(13)	-82.01(10)
P(2)-Fe(1)-P(1)-C(13)	10.59(7)
N(2)-Fe(1)-P(1)-C(17)	-101.75(11)
N(1)-Fe(1)-P(1)-C(17)	40.24(12)
P(2)-Fe(1)-P(1)-C(17)	132.84(10)
N(2)-Fe(1)-P(1)-C(15)	26.18(9)
N(1)-Fe(1)-P(1)-C(15)	168.17(10)
P(2)-Fe(1)-P(1)-C(15)	-99.24(7)
N(2)-Fe(1)-P(2)-C(19)	173.06(9)
N(1)-Fe(1)-P(2)-C(19)	33.18(9)
P(1)-Fe(1)-P(2)-C(19)	-95.01(8)
N(2)-Fe(1)-P(2)-C(21)	46.38(11)
N(1)-Fe(1)-P(2)-C(21)	-93.50(11)
P(1)-Fe(1)-P(2)-C(21)	138.31(10)
N(2)-Fe(1)-P(2)-C(14)	-78.34(9)
N(1)-Fe(1)-P(2)-C(14)	141.79(8)
P(1)-Fe(1)-P(2)-C(14)	13.60(7)
C(17)-P(1)-C(13)-C(14)	179.47(15)
C(15)-P(1)-C(13)-C(14)	73.22(16)
Fe(1)-P(1)-C(13)-C(14)	-39.77(16)
P(1)-C(13)-C(14)-P(2)	54.56(18)
C(19)-P(2)-C(14)-C(13)	71.65(16)
C(21)-P(2)-C(14)-C(13)	177.46(14)
Fe(1)-P(2)-C(14)-C(13)	-42.28(15)
C(13)-P(1)-C(15)-C(16)	56.69(19)
C(17)-P(1)-C(15)-C(16)	-46.44(19)
Fe(1)-P(1)-C(15)-C(16)	170.32(16)
C(13)-P(1)-C(17)-C(18)	-169.40(18)
C(15)-P(1)-C(17)-C(18)	-63.97(19)
Fe(1)-P(1)-C(17)-C(18)	65.2(2)
C(21)-P(2)-C(19)-C(20)	55.41(19)
C(14)-P(2)-C(19)-C(20)	160.80(17)
Fe(1)-P(2)-C(19)-C(20)	-85.91(17)
C(19)-P(2)-C(21)-C(22)	45.9(2)
C(14)-P(2)-C(21)-C(22)	-58.4(2)

Fe(1)-P(2)-C(21)-C(22)	174.79(14)

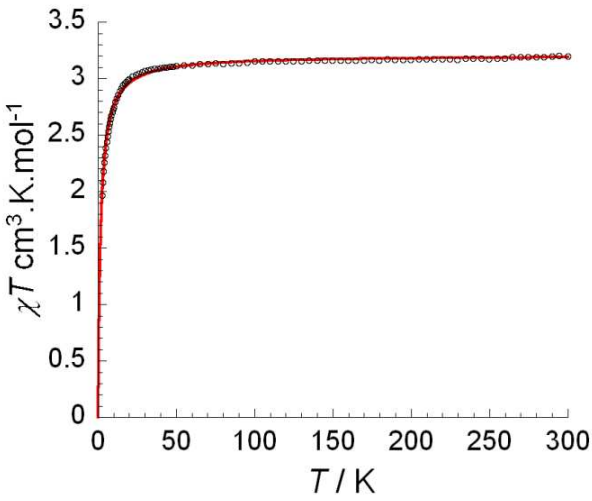

Figure S5. Temperature dependence of χT at 1000 Oe for **2**. The linear fit obeys the Curie-Weiss Law.

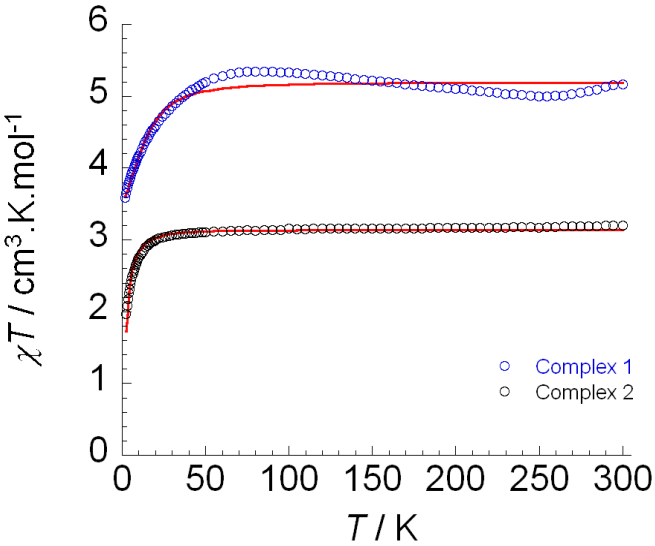

Figure S6. Fitting of the temperature dependence of χT data for **1** and **2** assuming a simple ZFS effect (employed fitting equation is shown below).

$$\chi_m = \frac{Ng^2\beta^2}{3kT} \times \left(\frac{2e^{-x} + 8e^{-4x}}{1 + 2e^{-x} + 2e^{-4x}} + 2 \times \frac{\left(\frac{6}{x}\right)(1 - e^{-x}) + \left(\frac{4}{3x}\right)(e^{-x} - e^{-4x})}{1 + 2e^{-x} + 2e^{-4x}}\right)$$

x = D/kT

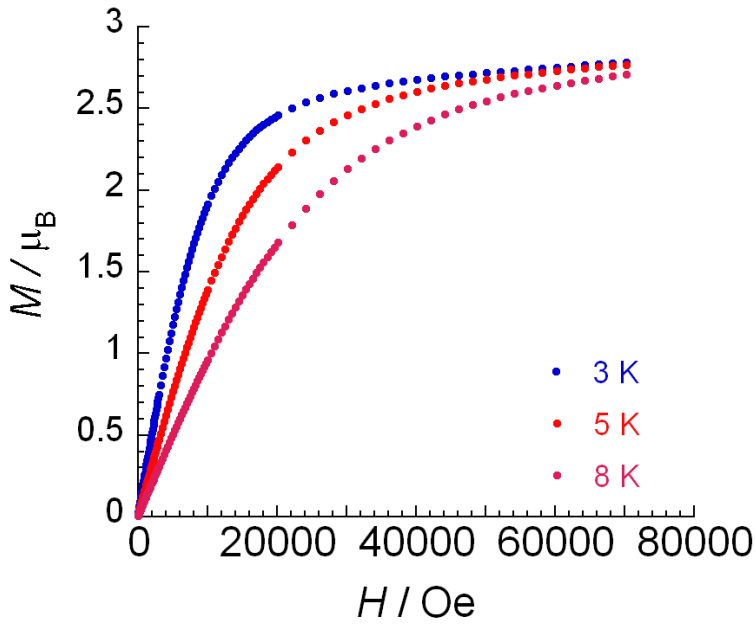

Figure S7. Field dependence of the magnetization, *M*, at 3, 5 and 8 K for **1**.

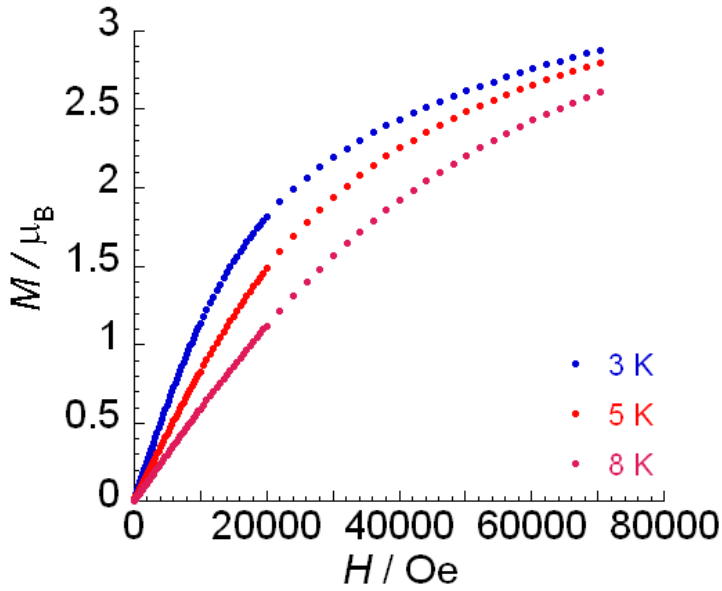

Figure S8. Field dependence of the magnetization, *M*, at 3, 5 and 8 K for **2**.

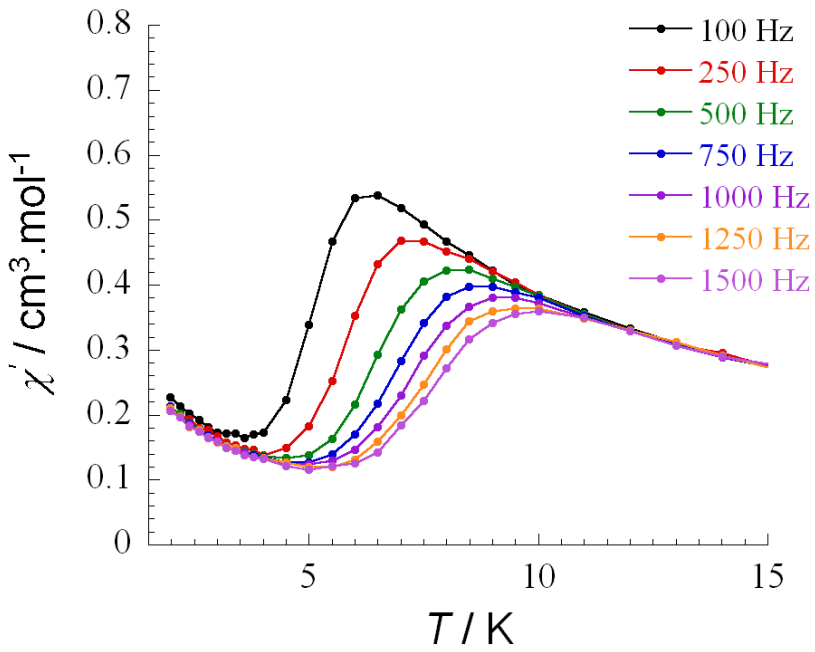

Figure S9. Frequency dependence of the in-phase magnetic susceptibility (χ') of **1** under an applied field of 600 Oe.

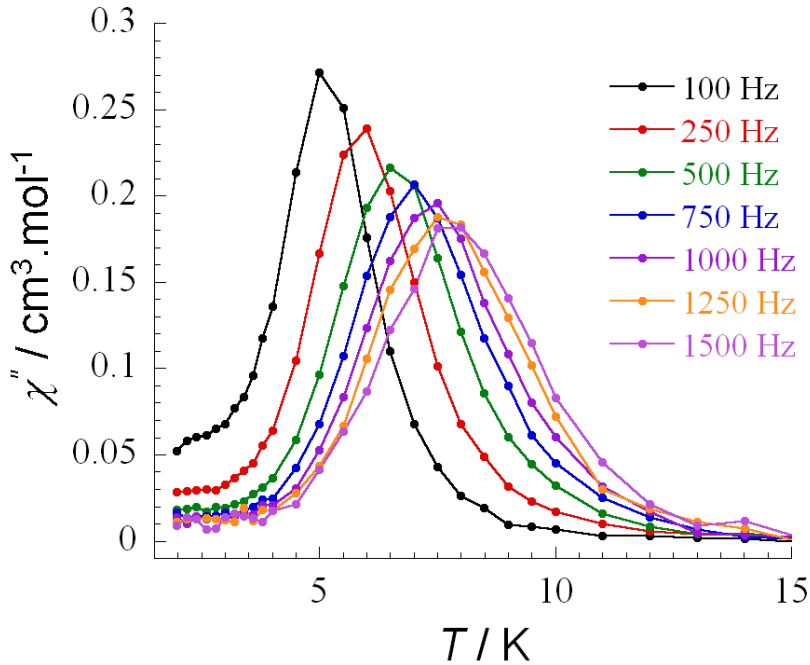

Figure S10. Frequency dependence of the out-of-phase magnetic susceptibility (χ'') of **1** under an applied field of 600 Oe.

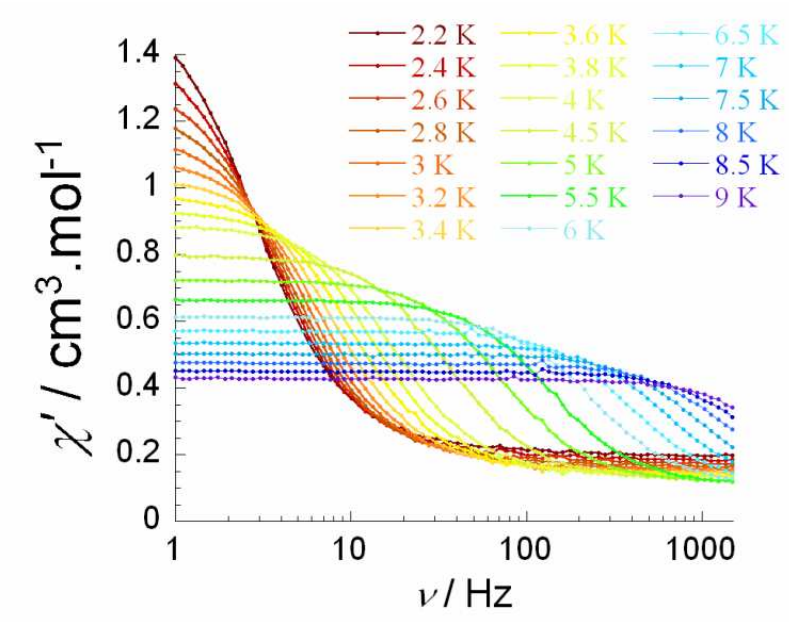

Figure S11. Temperature dependence of the in-phase magnetic susceptibility (χ') of **1** under an applied field of 600 Oe. Data were collected in temperature increments of 0.2 (2.2-3.8 K) and 0.5 (4.0-9.0 K) K.

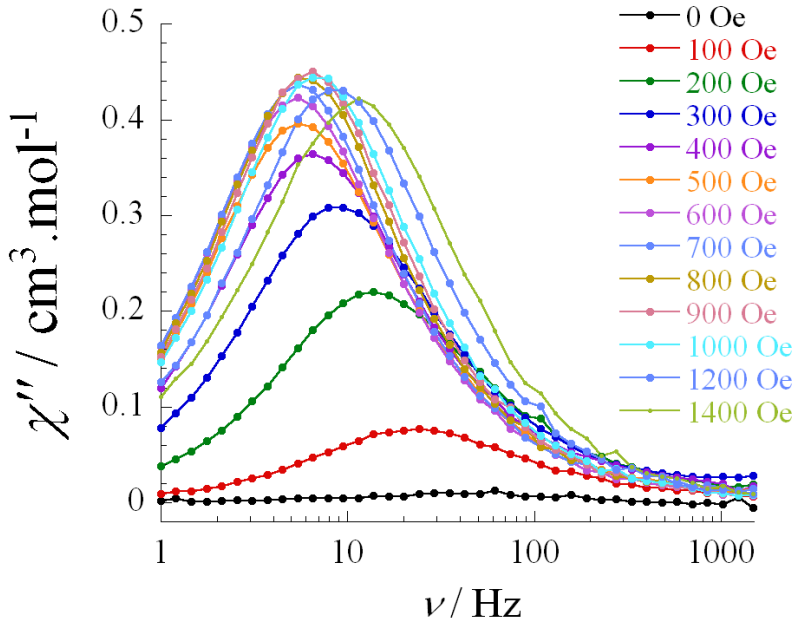

Figure S12. Field dependence of the out-of-phase magnetic susceptibility (χ'') of **1** in variable applied fields from 0 to 1400 Oe measured at 3 K.

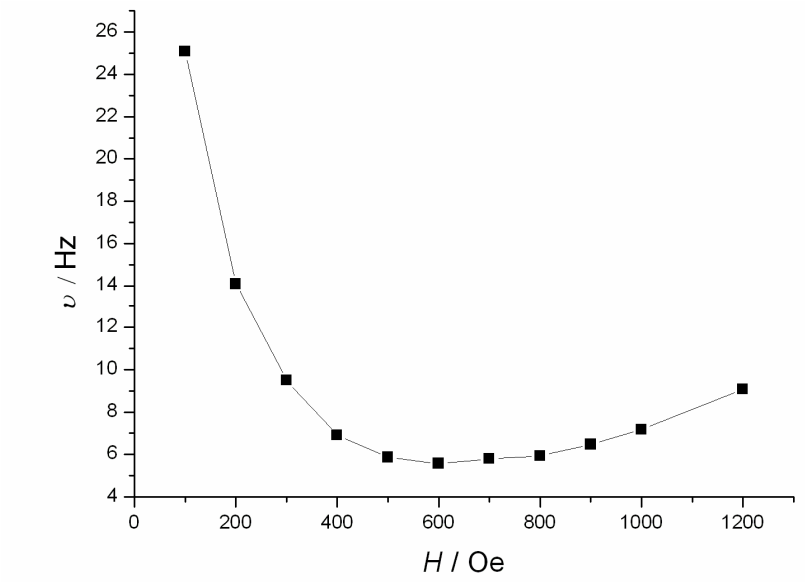

Figure S13. Field dependence of the characteristic frequency (maximum of χ'') as a function of the applied dc field for **1** at 3 K. Line is guide for the eyes.

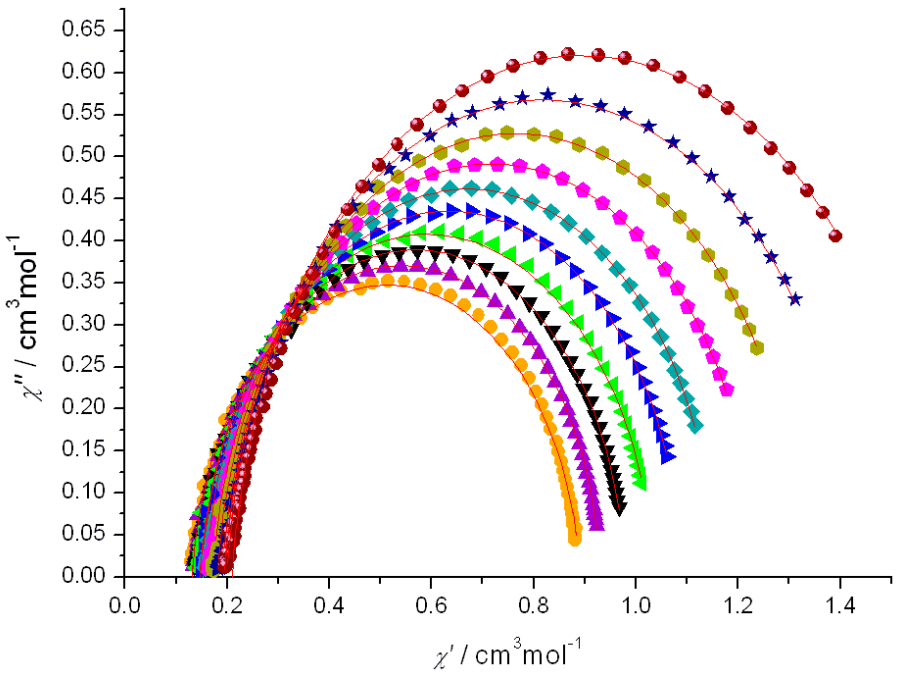

Figure S14. *Cole-Cole* plot for **1**, solid lines corresponds to the fit for a single relaxation process.

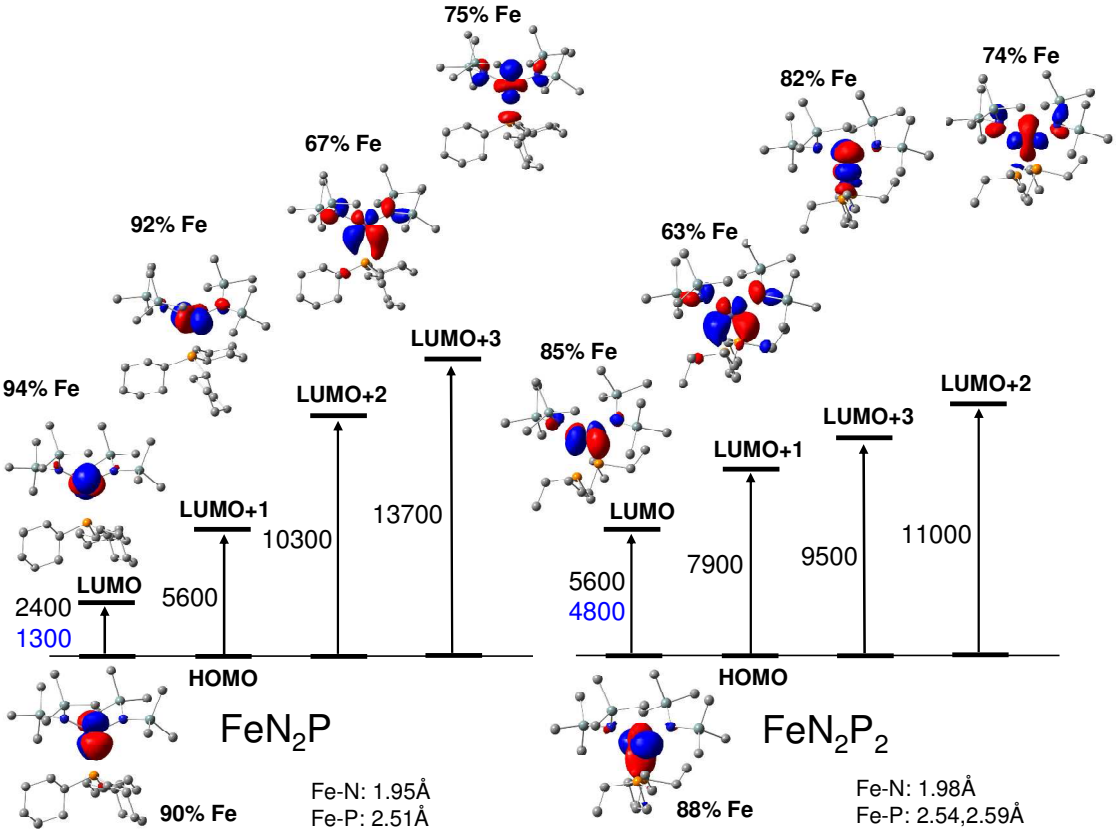

Figure S15. TD-DFT calculated four lowest-energy excited states and the molecular orbitals involved in the excitations for complexes **1** (left) and **2** (right). The excited state energies (cm^{-1}) from PBE and B3LYP calculations are shown in black and blue, respectively. The percent contributions of the Fe atom to the density of molecular orbitals are also shown.

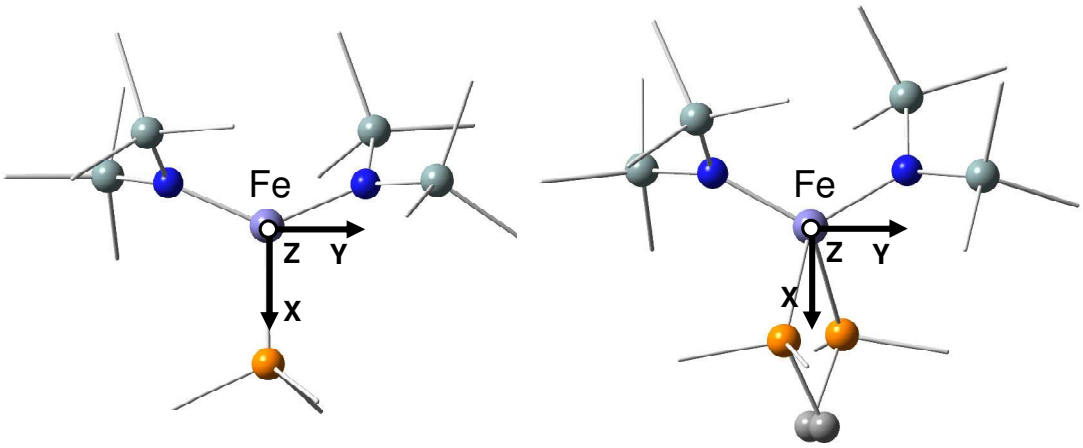

Figure S16. Orientation of the Cartesian axes with respect to the molecular frame of complexes **1** (left) and **2** (right). Functional groups on the ligands are removed for simplicity.

Table S12. Comparison of experimental and calculate geometric parameters (bond lengths, r, and bond angles, θ) for high-spin (quintet) states of complexes **1** and **2**

	Complex **1**	
	X-ray structure	Calculated (quintet)
r(Fe-N) (Å)	1.95	1.95
r(Fe-P) (Å)	2.52	2.51
θ(N-Fe-N) (^{o})	128.5	133.1
sum of angles around Fe	359.9	359.9
	Complex **2**	
r(Fe-N) (Å)	1.99, 2.00	1.98
r(Fe-P) (Å)	2.59, 2.60	2.54, 2.59
θ(N-Fe-N) (^{o})	120.9	121.1
θ(P-Fe-P) (^{o})	78.4	80.4

References

[1] APEX II 1.08, **2004**, Bruker AXS, Inc., Madison, Wisconsin 53719.

[2] SAINT+ 7.06, **2003**, Bruker AXS, Inc., Madison, Wisconsin 53719.

[3] SADABS 2.03, **2001**, George Sheldrick, University of Göttingen, Germany.

[4] SHELXTL 5.10, **1997**, Bruker AXS, Inc., Madison, Wisconsin 53719.

[5] Farrugia, L. J. *J. Appl. Cryst.* **1997**, *30*, 565.

[6] Gaussian 09, Revision A.02, Frisch, M. J.; Trucks, G. W.; Schlegel, H. B.; Scuseria, G. E.; Robb, M. A.; Cheeseman, J. R.; Scalmani, G.; Barone, V.; Mennucci, B.; Petersson, G. A.; Nakatsuji, H.; Caricato, M.; Li, X.; Hratchian, H. P.; Izmaylov, A. F.; Bloino, J.; Zheng, G.; Sonnenberg, J. L.; Hada, M.; Ehara, M.; Toyota, K.; Fukuda, R.; Hasegawa, J.; Ishida, M.; Nakajima, T.; Honda, Y.; Kitao, O.; Nakai, H.; Vreven, T.; Montgomery, Jr., J. A.; Peralta, J. E.; Ogliaro, F.; Bearpark, M.; Heyd, J. J.; Brothers, E.; Kudin, K. N.; Staroverov, V. N.; Kobayashi, R.; Normand, J.; Raghavachari, K.; Rendell, A.; Burant, J. C.; Iyengar, S. S.; Tomasi, J.; Cossi, M.; Rega, N.; Millam, J. M.; Klene, M.; Knox, J. E.; Cross, J. B.; Bakken, V.; Adamo, C.; Jaramillo, J.; Gomperts, R.; Stratmann, R. E.; Yazyev, O.; Austin, A. J.; Cammi, R.; Pomelli, C.; Ochterski, J. W.; Martin, R. L.; Morokuma, K.; Zakrzewski, V. G.; Voth, G. A.; Salvador, P.; Dannenberg, J. J.; Dapprich, S.; Daniels, A. D.; Farkas, Ã–.;Foresman, J. B.; Ortiz, J. V.; Cioslowski, J.; Fox, D. J. *Gaussian, Inc*., *Wallingford* CT, **2009**.

[7] Schafer, A.; Huber, C.; Ahlrichs, R. *J. Chem. Phys*. **1994**, *100*, 5829.

[8] Perdew, J. P.; Burke, K.; Ernzerhof, M. *Phys. Rev. Lett.* **1997**, *78*, 1396.

[9] (a) Becke, A. D. *J. Chem. Phys*. **1993**, *98*, 5648. (b) Lee, C.; Yang, W.; Parr, R. G. *Phys. Rev. B* **1988**, *37*, 785.

[10] Stratmann, R. E.; Scuseria, G. E.; Frisch, M. J. *J. Chem. Phys*. **1998**, *109*, 8218.

[11] Reed, A. E.; Weinstock, R. B.; Weinhold, F. *J. Chem. Phys*. **1985**, *83*, 735.

[12] (a) Mayer, I. *Int. J. Quantum Chem*. **1986**, *29*, 73. (b) Gorelsky, S. I.; Basumallick, L.; Vura-Weis, J.; Sarangi, R.; Hedman, B.; Hodgson, K. O.; Fujisawa, K.; Solomon, E. I. *Inorg. Chem*. **2005**, *44*, 4947.

[13] Mulliken, R. S. *J. Chem. Phys*. **1955**, *23*, 1833.

[14] (a) Gorelsky, S. I. *AOMix* – Software for Electronic Structure Analysis; Centre for Catalysis Research and Innovation, Department of Chemistry, University of Ottawa: Ottawa, ON, 2011; http://www.sg-chem.net.(b) Gorelsky, S. I.; Lever, A. B. P. *J. Organomet. Chem*. **2001**, *635*, 187.